Water-Soluble Copolymers. 56. Structure and Solvation Effects of Polyampholytes in Drag Reduction

Pavneet S. Mumick, Paul M. Welch, Luis C. Salazar, and Charles L. McCormick*

Department of Polymer Science, The University of Southern Mississippi, Southern Station, Box 10076, Hattiesburg, Mississippi 39406-0076

Received June 7, 1993; Revised Manuscript Received October 27, 1993®

ABSTRACT: Water-soluble polyampholytes based on acrylamide (AM), sodium 2-acrylamido-2-methylpropanesulfonate (NaAMPS), (2-acrylamido-2-methylpropyl)trimethylammonium chloride (AMPTAC), sodium 3-acrylamido-3-methylbutanoate (NaAMB), and 3-((2-acrylamido-2-methylpropyl)dimethylammonio)-1-propanesulfonate (AMPDAPS) have been synthesized and characterized. The molecular weights of the polymers range from 1.4×10^6 to 21.5×10^6. Almost all the polyampholytes showed higher intrinsic viscosities at higher solvent ionic strength. The drag reduction behavior of high and low charge density polyampholytes and polybetaines was examined with a rotating-disk rheometer. All the polymers exhibited higher drag reduction at increased solvent ionic strength. The poly(sulfobetaines) (copolymers of AM and AMPDAPS) were found to be the most efficient drag reducers, and the high charge density polyampholyte (copolymer containing 50 mol % each of AMPTAC and NaAMPS) was the least efficient. Experimental data indicate that theoretical models of drag reduction should include parameters for polymer–solvent interactions and molecular associations.

Introduction

It is well known that certain additives can reduce the energy loss due to friction in turbulent flow. Toms first reported this drag reduction phenomenon in 1949.[1] The most effective drag-reducing additives are high molecular weight polymers. Some empirical models have accurately predicted the drag reduction behavior of water-soluble homopolymers such as poly(ethylene oxide) and polyacrylamide. However, despite the plethora of theoretical, experimental, and practical studies of the phenomenon[7,17] over the past 40 years, there is no comprehensive, universally accepted model which explains the drag reduction mechanism(s). The role of polymer microstructure and solvation is particularly unclear.

The interrelated molecular parameters which affect drag reduction performance are molecular weight, molecular weight distribution, chemical nature of the polymer, branching and co- and terpolymer composition, concentration, solvent quality, hydrodynamic size, second viral coefficient, entanglements, and energetic interactions (i.e., associations, aggregations, and hydrogen bonding).

The drag reduction properties of several polymers of widely differing structures and compositions have been extensively analyzed in our research group.[2–8] All the polymer models were found to conform to a universal curve for drag reduction when normalized for hydrodynamic volume fraction of polymer in solution.[2,3,5–8] This method of data analysis allows the facile comparison of drag reduction efficiencies (DRE) of polymers of widely differing structures, compositions, and molecular weights. The most efficient drag reducers are polymers which yield the greatest values of (% DR/$[\eta]C$) at a particular hydrodynamic volume fraction (e.g., $[\eta]C = 0.001$). The DRE appears to be related to the efficiency with which the polymer hydrodynamic coil interacts with and disrupts the microvortices present in turbulent flow. We have further normalized DRE values relative to poly(ethylene oxide) (PEO) by incorporating a parameter, Δ, to yield one universal curve. Δ values > 1 indicate more efficient drag reduction than that of PEO, and $\Delta < 1$ denotes decreased drag reduction efficiency relative to PEO.[3,5–8] Virk[9] developed a universal drag reduction relationship which was later rearranged by Little.[10] This relationship, which accounts for the concentration dependence of drag reduction, takes the form

$$\frac{C}{\mathrm{DR}} = \frac{[C]}{\mathrm{DR}_{\max}} + \frac{C}{\mathrm{DR}_{\max}} \tag{1}$$

at a fixed Reynolds number, where C = concentration in ppm, DR = percent drag reduction, $\mathrm{DR}_{\max}$ = maximum drag reduction, and $[C]$ = intrinsic concentration in ppm. The intrinsic concentration is defined by

$$[C] = \frac{\mathrm{DR}_{\max}}{\lim_{C\to 0}(\mathrm{DR}/C)} \tag{2}$$

The quantity in the denominator is the intrinsic drag reduction, which is a measure of the drag reduction per unit concentration at infinite dilution. $[C]$ is inversely related to molecular weight.[11] The effect of polymer–solvent interactions on $[C]$ has not been directly addressed in the literature.

Most of the theories for drag reduction are interrelated and include variations of the idea that polymer molecules interact with vortices that are formed in turbulent flow and dissipate energy necessary for the vortices to grow. This energy may be dissipated through breakage of primary or secondary bonds, through conformational changes, through associations/dissociations, by inducing changes in the solvent structure around the macromolecules, or by other mechanisms.[2,7,17] Many theories also include the concept that the polymer molecules act near the wall in the boundary layer.

Walsh[12] developed a model based on the energy storage capability of a polymer and associated solvent. He suggested that the polymer molecules alter the energy balance by interacting with microvortices as they form near the wall, thereby preventing their growth. Walsh defined a dimensionless parameter, H, as a measure of the effect of polymer additives on the rate of diffusion of

* Abstract published in *Advance ACS Abstracts,* December 15, 1993.

0024-9297/94/2227-0323$04.50/0

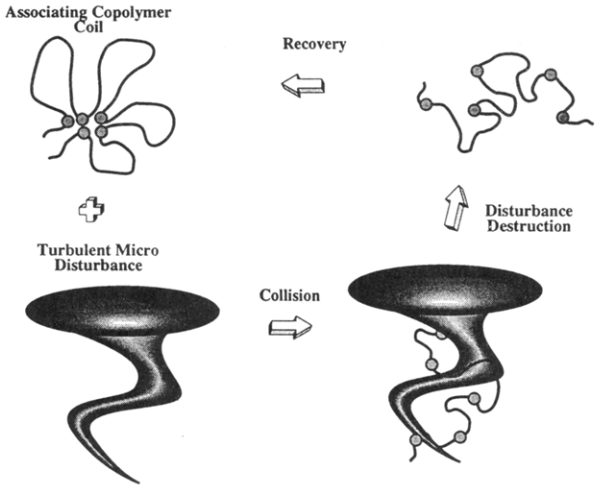

Figure 1. Reduction of turbulence by an associating polymer coil.

turbulence near the wall

$$H = \frac{8CM[\eta]^2 T_w}{RT} \tag{3}$$

where C = polymer concentration, M = molecular weight, $[\eta]$ = intrinsic viscosity, T_w = wall shear stress, R = the gas constant, and T = temperature. Onset of drag reduction was predicted at $H \simeq 0.01$ and maximum drag reduction at $H \simeq 1$.

Lumley[13] suggested that in turbulence polymer elongation leads to substantially increased viscosity in a fluid layer near the wall. Turbulent eddies are damped in this layer of increased viscosity, leading to reduced momentum transport from the buffer zone. Ryskin[14,15] developed a predictive model based on Lumley's ideas and his own "yo-yo" model of polymer dynamics. The polymer effect on viscosity enhancement, ζ_{turb}, is given by the expression

$$\zeta_{turb} \simeq \frac{0.05\alpha^3 N_A a^3 N^2 C}{M_a} \tag{4}$$

where N_A = Avogadro's number, a = length of a repeat unit, N = degree of polymerization, C = polymer concentration, M_a = molecular weight per repeat unit, and α = ratio of chain length to that of a fully extended chain. Ryskin related ζ_{turb} to percent drag reduction and to Virk's[16] slope increment, which is a measure of drag reduction effectiveness. To accurately assess the validity of these vastly different models, further correlation with experimental data is required.

Since only a few parts per million of polymer additives are involved in the drag reduction phenomenon, it seems logical to hypothesize that polymer–solvent interactions play a very important role. Therefore, we have designed studies to test this idea. Experimental evidence in our laboratory indicates that changes in conformational structure and associated solvent affect drag reduction behavior.[2-5] Recently,[7,8] we have synthesized polymers which might enhance drag reduction by an association/dissociation mechanism depicted in Figure 1. An associating polymer coil interacts with a turbulent microdisturbance and disrupts this disturbance by absorbing its energy and in the process becomes dissociated. On moving out of the turbulent regime, this dissociated macromolecule reverts back to its associated state and once again goes through the above process. The polymer and bound solvent are likely involved in energy dissipation.

This paper reports the study of drag reduction behavior of water-soluble polyampholytes of widely differing structures and compositions. Polyampholytes are a class of polymers which contain both positive and negative charges on the same macromolecular chain. These polymers exhibit what has been termed an "antipolyelectrolyte" behavior in solution; i.e., higher intrinsic viscosities are observed with increasing solvent ionic strength. We have studied high and low charge density polyampholytes as well as sulfobetaine copolymers. The hydrodynamic volume and solution properties of these copolymers are extremely sensitive to ionic strength, making them good models to assess the effect of polymer–solvent interaction on drag reduction performance.

Table 1. Copolymer and Terpolymer Compositions (mol %)[7,18]

polymer	AM	Na-AMPS	Na-AMB	AMPTAC	AMPDAPS
PAM	100.0				
ATAS-50		48.3		51.7	
ATASAM 5–5	86.1	6.9		7.0	
ATASAM 10–10	76.0	11.9		12.1	
ATABAM 0.5–0.5	99.0[a]		0.5[a]	0.5[a]	
ATABAM 2.5–2.5	89.1		5.1	5.8	
ATABAM 15–15	74.5		11.5	14.0	
DAPS-10	90.0				10.0
DAPS-40	61.1				38.9

[a] Theoretical.

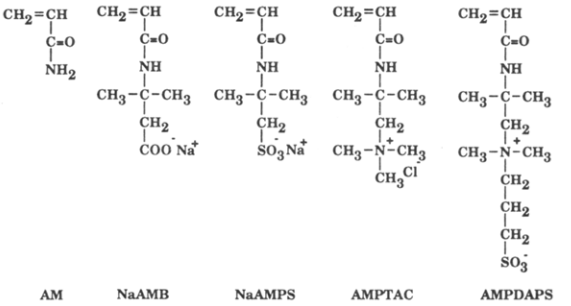

Experimental Section

Monomer and Polymer Synthesis. The polyampholytes were synthesized using the comonomers acrylamide (AM), sodium 2-acrylamido-2-methylpropanesulfonate (NaAMPS), (2-acrylamido-2-methylpropyl)trimethylammonium chloride (AMPTAC), sodium-3-acrylamido-3-methylbutanoate (NaAMB), and 3-((2-acrylamido-2-methylpropyl)dimethylammonio)-1-propanesulfonate (AMPDAPS) (Table 1). AM and NaAMPS were obtained from Aldrich and Fluka, respectively. The syntheses of NaAMB, AMPTAC, and AMPDAPS have been outlined elsewhere.[18-22] The monomers were free-radically polymerized in 0.5 M NaCl solution using 0.1 mol % potassium persulfate as initiator at 30 °C under a nitrogen atmosphere. The total monomer concentration was held constant at 0.45 M for all the co- and terpolymerizations. The use of 0.5 M NaCl as the reaction medium ensured that polymers with high charge content remained in homogeneous solution during polymerization. Details of the polymerization technique and polymer purification are outlined elsewhere.[18-22]

Polymer Characterization and Dilute Solution Properties. ^{13}C NMR and elemental analysis (M-H-W Laboratories, Phoenix, AZ) were used to determine co- and terpolymer compositions. The molecular weight studies were performed on a Chromatix KMX-6 low-angle laser light scattering spectrophotometer utilizing a 2-mW He–Ne laser operating at 633 nm. Specific refractive index increments, dn/dc, were measured on a Chromatix KMX-16 laser differential refractometer. The viscosity measurements were made on a Contraves LS-30 rheometer at a shear rate of 6.0 s^{-1}.

Drag Reduction Measurements. The drag reduction measurements were performed with a rotating-disk rheometer[23] consisting of a 9-cm-radius circular disk rotating in a 18.5-L cylindrical chamber. The percent drag reduction (% DR) was

Table 2. Low-Angle Laser Light Scattering Data in 1 M NaCl at 25 °C[7,18]

polymer	$M_w \times 10^{-6}$	$A_2 \times 10^4$ (mL·mol/g^2)	$DP_w \times 10^{-4}$
PEO(WSR-N-60K)	3.0[a]		6.82
PAM[b]	5.2	3.78	7.31
ATAS-50	7.7	0.76	3.52
ATASAM 5–5	5.1	2.00	5.48
ATASAM 10–10	5.9	1.57	5.44
ATABAM 2.5–2.5	13.9	1.66	15.0
ATABAM 15–15	12.2	1.75	11.5
DAPS-10	21.5	1.49	23.0
DAPS-40	17.5	1.21	11.0
ATABAM 0.5–0.5	1.4	3.68	1.97

[a] As reported by Union Carbide. [b] In deionized water.

calculated by comparing the torque on the disk in the solvent to that in the polymer solution:

$$\% \text{ DR} = 100 \times \frac{T_s - T_p}{T_s} \quad (5)$$

where T_s = torque in the solvent and T_p = torque in the polymer solution. The Reynolds number (Re) and friction factor (f) were calculated from the following equations:

$$Re = \frac{\rho R^2 \omega}{\mu} \quad (6)$$

$$f = \frac{T}{\pi R^5 \rho \omega^2} \quad (7)$$

where ρ = fluid density, μ = fluid viscosity, R = radius of the disk, ω = angular velocity of the disk, and T = torque on the disk.

Polymer stock solutions were prepared at room temperature by dissolving the polymer and 0.01% sodium azide, a biocide, in solvent in 500-mL flasks by gentle stirring for 3–4 days. These stock solutions were then aged for 1 week. The required amount of the stock solution was then measured and directly added to the rotating-disk rheometer and was allowed to mix with the solvent for 3 min at low disk rotational speed (~100 rpm) to avoid any shear degradation of polymer. The drag reduction measurements were conducted at 23 °C.

Results and Discussion

Polymer Characterization. All copolymers and terpolymers show random incorporation of their respective monomers with the exception of ATAS-50 (copolymer containing 50 mol % each of AMPTAC and NaAMPS), which shows a slight tendency toward alternation.[18,19] The co- and terpolymer compositions of the various polyampholytes are reported in Table 1.

ATAS-50, the high charge density polyampholyte, has 48.3 mol % NaAMPS and 51.7 mol % AMPTAC incorporated into the copolymer. The low charge density ATASAM terpolymers (terpolymer of AM, NaAMPS, and AMPTAC) have slightly higher amounts of the charged monomers incorporated into the copolymer relative to the feed compositions. Likewise, ATABAM 2.5–2.5 (terpolymer of AM, NaAMB, and AMPTAC) also has more incorporation of the charged monomers relative to the feed composition, whereas ATABAM 15–15 has less incorporation of the charged monomers in the copolymer. Sulfobetaine copolymers DAPS-10 and DAPS-40 have copolymer compositions approaching those in the feed.

Light scattering data for all polymers are reported in Table 2. The molecular weights range from 1.4×10^6 to 21.5×10^6. The second virial coefficient (A_2), which is a measure of polymer–solvent interaction, decreases with increasing charge content for the polyampholytes in 1 M NaCl. The lowest value is observed for ATAS-50, which is a high charge density polyampholyte and very poorly hydrated, and the highest value is observed for polyacrylamide (PAM). The low charge density ATASAM and ATABAM terpolymers and the zwitterionic DAPS copolymers have intermediate A_2 values.

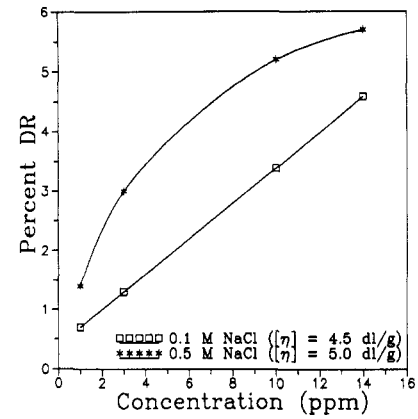

Figure 2. Percent DR versus concentration for ATAS-50 in 0.1 M (□) and 0.5 M NaCl (*) at T_w = 1122 dyn/cm^2 in the rotating-disk rheometer.

Table 3. Percent Drag Reduction for 3 ppm Solutions of Different Polymer/Solvent Systems at T_w = 1122 dyn/cm^2 in the Disk

polymer/solvent	% DR for a 3 ppm solution
PEO(WSR-N-60K)/DI water	14.2
ATAS-50/0.1 M NaCl	1.3
ATAS-50/0.5 M NaCl	3.0
ATASAM 5–5/DI water	1.6
ATASAM 5–5/0.5 M NaCl	7.2
ATASAM 10–10/0.1 M NaCl	4.9
ATASAM 10–10/0.5 M NaCl	7.3
ATABAM 0.5–0.5/DI water	4.9
ATABAM 0.5–0.5/0.5 M NaCl	5.9
ATABAM 2.5–2.5/DI water	13.1
ATABAM 2.5–2.5/0.5 M NaCl	21.2
ATABAM 15–15/0.05 M NaCl	15.4
ATABAM 15–15/0.5 M NaCl	17.9
DAPS-10/DI water	27.1
DAPS-10/0.5 M NaCl	31.0
DAPS-40/DI water	8.1
DAPS-40/0.5 M NaCl	15.5

Dilute Solution and Drag Reduction Properties. The dilute solution and drag reduction properties of the various polyampholytes[18–22] were measured as a function of solvent ionic strength. The drag reduction measurements have been made at an outer wall shear stress (T_w) of 1122 dyn/cm^2 and a disk Reynolds number of approximately 850 000, which corresponds to a disk rotational speed of 1000 rpm.

Sulfonate-Containing Polyampholytes. Figure 2 illustrates the drag reduction profiles and intrinsic viscosities for ATAS-50 as a function of solvent ionic strength. ATAS-50 is insoluble in deionized water due to very strong intramolecular ionic associations. Less water is associated with the polymer due to strong charge attractions between oppositely charged ions. Even in 0.1 M NaCl, the percent drag reduction (% DR) is small due to remaining intramolecular associations (Table 3). The % DR and intrinsic viscosity increase slightly with increasing solvent ionic strength.

ATASAM 5–5 (Figure 3) exhibits a large increase in % DR as well as hydrodynamic volume when the solvent is changed from deionized water to 0.5 M NaCl. In this case, unlike for ATAS-50, solvent ionic strength is effective in disrupting the intramolecular ionic associations. In 0.5 M NaCl, ATASAM 5–5 shows a higher % DR than ATAS-50 (Table 3).

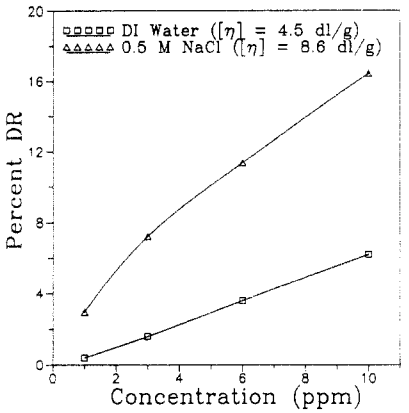

Figure 3. Percent DR versus concentration for ATASAM 5–5 in deionized water (□) and 0.5 M NaCl (△) at T_w = 1122 dyn/cm² in the rotating-disk rheometer.

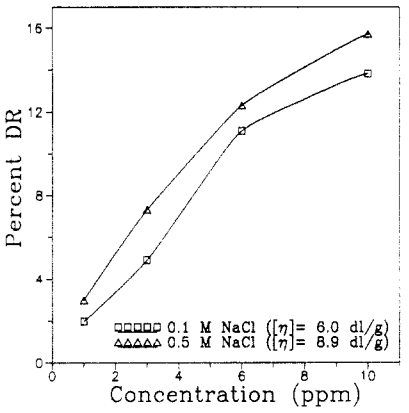

Figure 4. Percent DR versus concentration for ATASAM 10–10 in 0.1 M (□) and 0.5 M NaCl (△) at T_w = 1122 dyn/cm² in the rotating-disk rheometer.

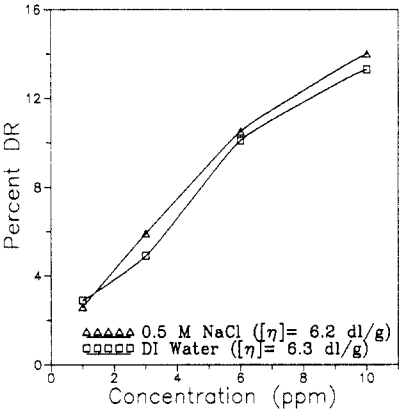

Figure 5. Percent DR versus concentration for ATABAM 0.5–0.5 in deionized water (□) and 0.5 M NaCl (△) at T_w = 1122 dyn/cm² in the rotating-disk rheometer.

ATASAM 10–10 is insoluble in deionized water and, hence, is studied in 0.1 M NaCl. The intrinsic viscosity increases from 6.0 to 8.9 dL/g as the NaCl concentration is increased from 0.1 to 0.5 M (Figure 4). However, the effect of ionic strength on % DR is much smaller. In 0.5 M NaCl, ATASAM 5–5 and ATASAM 10–10 show similar percent drag reduction (Table 3).

Carboxylate-Containing Polyampholytes. ATABAM 0.5–0.5 (Figure 5), which contains only 0.5 mol % each of the charged comonomers, exhibits almost no change in percent drag reduction or hydrodynamic volume with increasing solvent ionic strength. Thus, the polyampholyte effect is unimportant at such low incorporation of the charged comonomers. The low % DR (Table 3) can be attributed to the relatively low molecular weight.

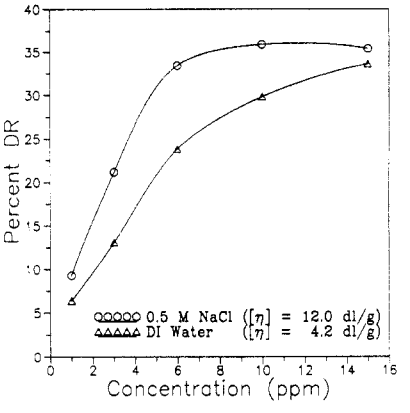

Figure 6. Percent DR versus concentration for ATABAM 2.5–2.5 in deionized water (△) and 0.5 M NaCl (○) at T_w = 1122 dyn/cm² in the rotating-disk rheometer.

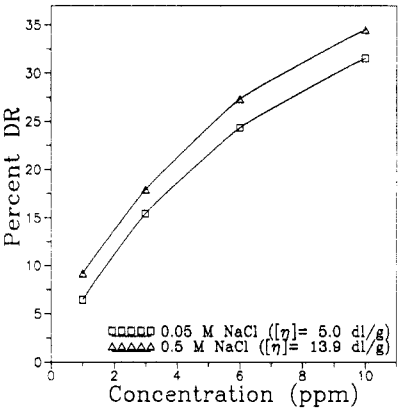

Figure 7. Percent DR versus concentration for ATABAM 15–15 in 0.05 M (□) and 0.5 M NaCl (△) at T_w = 1122 dyn/cm² in the rotating-disk rheometer.

ATABAM 2.5–2.5 (Figure 6) exhibits a large increase in intrinsic viscosity with an increase in solvent ionic strength (4.2 dL/g in deionized water and 12.0 dL/g in 0.5 M NaCl). However, the increase in percent drag reduction is not as substantial. This is possibly due to the different shear rates the polymer experiences during viscosity measurements relative to the drag reduction measurements. In the viscosity studies, in deionized water, the intramolecular ionic associations are strong enough that they are not disrupted under zero-shear conditions, resulting in low intrinsic viscosities. Upon the addition of sodium chloride these associations are disrupted, resulting in a large increase in intrinsic viscosity. During drag reduction measurements in deionized water, the polymer experiences much higher shear rates, resulting in the disruption of some of the intramolecular associations. Therefore, upon the addition of 0.5 M NaCl, the increase in % DR is not as substantial since there are not as many intramolecular ionic associations to disrupt. The % DR for ATABAM 2.5–2.5 is higher than that for the ATASAM and ATAS polymers (Table 3), also indicating weaker intramolecular ionic associations in the ATABAM terpolymers relative to the ATASAM and ATAS polyampholytes. If one considers "hard–soft acid–base" theory,[24,25] the carboxylate anion is hard, the sulfonate anion is soft, and the quaternary ammonium cation is soft. Accordingly, the intramolecular ionic associations should be weak in the ATABAM terpolymers and strong in the ATASAM and ATAS copolymers.

ATABAM 15–15 (Figure 7) is insoluble in deionized water and, hence, has been studied in 0.05 M NaCl. Like ATABAM 2.5–2.5, this terpolymer also exhibits a large increase in intrinsic viscosity but only a small increase in

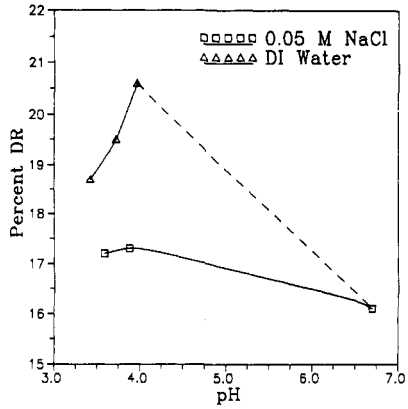

Figure 8. Percent DR versus pH for a 3 ppm solution of ATABAM 15–15 in deionized water (△) and 0.05 M NaCl (□) at T_w = 1122 dyn/cm² in the rotating-disk rheometer.

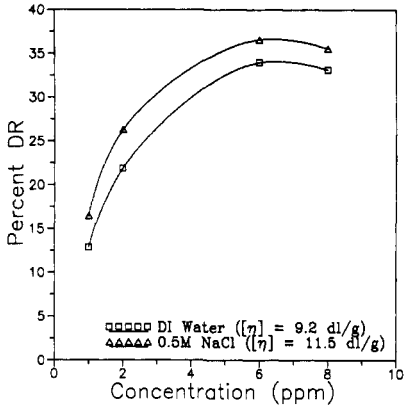

Figure 9. Percent DR versus concentration for DAPS-10 in deionized water (□) and 0.5 M NaCl (△) at T_w = 1122 dyn/cm² in the rotating-disk rheometer.

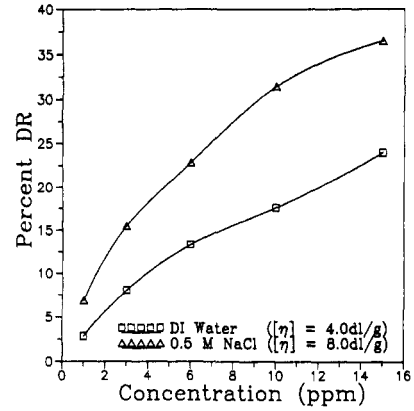

Figure 10. Percent DR versus concentration for DAPS-40 in deionized water (□) and 0.5 M NaCl (△) at T_w = 1122 dyn/cm² in the rotating-disk rheometer.

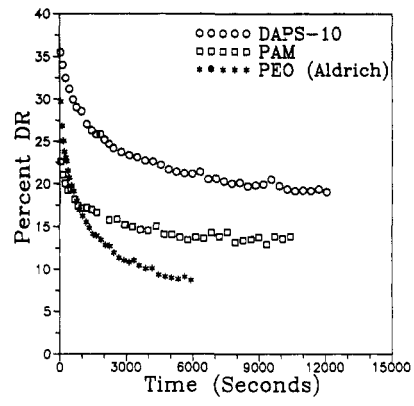

Figure 11. Degradation profile for 3 ppm solutions of different polymers in 0.5 M NaCl at T_w = 1122 dyn/cm² in the rotating-disk rheometer.

% DR with increasing solvent ionic strength. ATABAM 15–15 (despite the high charge density) shows comparable percent drag reduction relative to ATABAM 2.5–2.5 (Table 3), consistent with ionic associations in the ATABAM terpolymers being weaker than those in the ATASAM or ATAS polymers. These associations may be important in extension of the ATABAM terpolymers in turbulence.

pH Studies with the Carboxylate-Containing Polyampholytes. In deionized water (pH ~ 6.8), the NaAMB units possess a negative charge; at lower pH (~4.0) the NaAMB units are protonated. Therefore, when the ATABAM terpolymers are titrated to a pH of 4.0, only the cationic charge on the AMPTAC unit remains, and the polymers behave as polyelectrolytes. Figure 8 shows % DR versus pH for a 3 ppm solution of ATABAM 15–15 in deionized water and 0.005 M NaCl. The pH of the solution is lowered by addition of concentrated HCl. ATABAM 15–15 is insoluble in deionized water. Therefore, in deionized water, the part of the curve between pH 4 and pH 7 is depicted by a dashed line. When the pH decreases from 6.8 to 4.0, the drag reduction increases from 16.1 to 20.6% as the polyampholyte is converted to a polycation. On further addition of HCl, the pH drops slightly but the counterion condensation or ion pairing of the chloride ion with the cationic AMPTAC unit appears to reduce the hydrodynamic volume, leading to a decrease in % DR. This trend continues upon further addition of HCl. In 0.05 M NaCl, the trend remains the same as in deionized water; however, the effect is suppressed due to the presence of NaCl. ATABAM 2.5–2.5 has a similar pH response.

Sulfobetaine Copolymers. DAPS-10 (Figure 9) has the best drag reduction properties among all the systems studied in this paper (Table 3). The differences in the intrinsic viscosities and % DR are small with increasing solvent ionic strength, indicating that the DAPS copolymers are not as collapsed at low ionic strength as the ampholytic terpolymers having similar charge densities. This may be due to the existence of intramer associations on the same repeating unit, which decreases the number of charged groups available for intramolecular association.[6,7,18] Such an effect would also enhance the ability of the polymer to undergo an association–dissociation mechanism (Figure 1), leading to more efficient drag reduction.

DAPS-40 (Figure 10), unlike DAPS-10, exhibits a large increase in intrinsic viscosity and % DR with increasing solvent ionic strength. The higher charge content in DAPS-40 relative to DAPS-10 leads to stronger intramolecular ionic associations which are effectively disrupted in the presence of NaCl. DAPS-40 is not as good a drag reducer as DAPS-10 but has DR properties similar to those of the ATABAM terpolymers in 0.5 M NaCl (Table 3).

Resistance to Degradation. The degradation profiles for 3 ppm solutions of different polymers in 0.5 M NaCl are reported in Figure 11. DAPS-10 and polyacrylamide (PAM) have much better resistance to shear degradation compared to poly(ethylene oxide) (PEO). DAPS-10 and PAM retain approximately 60% of their initial level of drag reduction after 100 min at 1000 rpm in the rotating disk. Under similar conditions PEO retains only 28.5% of its initial drag reduction.

Volume Fraction Normalization. As discussed in the Introduction, volume fraction normalization allows the facile comparison of drag reduction efficiencies (DRE) of polymers of widely differing structures, compositions, and molecular weights,[2,3,5–8] Figure 12 is a plot of percent

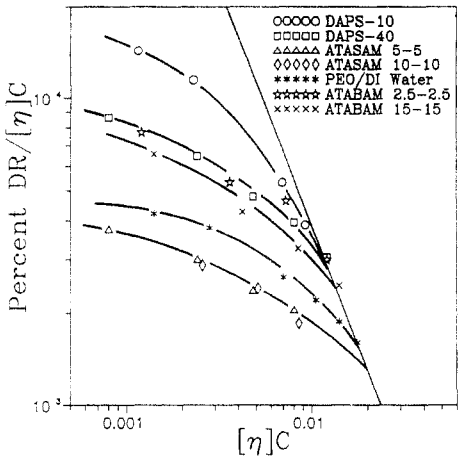

Figure 12. Percent DR per unit volume fraction versus volume fraction in 0.5 M NaCl at T_w = 1122 dyn/cm² in the rotating-disk rheometer.

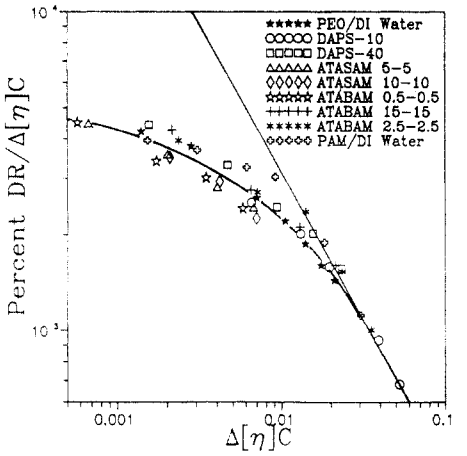

Figure 13. Percent DR per unit volume fraction versus volume fraction employing shift factors in 0.5 M NaCl at T_w = 1122 dyn/cm² in the rotating-disk rheometer.

Table 4. Relative Drag Reduction Efficiencies of Different Polymer/Solvent Systems

polymer/solvent	DR efficiency (Δ)
PEO(WSR-N-60K)/DI water	1.00
PAM/DI water	1.37
ATAS-50/0.5 M NaCl	0.45
ATASAM 5–5/0.5 M NaCl	0.84
ATASAM 10–10/0.5 M NaCl	0.82
ATABAM 0.5–0.5/0.5 M NaCl	0.93
ATABAM 2.5–2.5/0.5 M NaCl	1.96
ATABAM 15–15/0.5 M NaCl	1.54
DAPS-10/0.5 M NaCl	5.68
DAPS-40/0.5 M NaCl	1.95
ATAS-50/0.1 M NaCl	0.29
ATASAM 10–10/0.1 M NaCl	0.70
ATABAM 2.5–2.5/DI water	3.46
ATABAM 15–15/0.05 M NaCl	3.05
DAPS-10/DI water	4.64
DAPS-40/DI water	1.62

drag reduction per unit volume fraction versus polymer hydrodynamic volume fraction. The polymers which yield the greatest values of (% DR/[η]C) at a specific volume fraction (e.g., [η]C = 0.001) are the most efficient drag reducers. On further normalization using a Δ parameter (Figure 13), DRE values relative to poly(ethylene oxide) (PEO) have been determined. The drag reduction efficiency parameters (Δ) for the different polyampholytes in various solvents are listed in Table 4. The Δ parameter empirically demonstrates the effects of structure, composition, and solvent quality for the polymers in drag reduction.

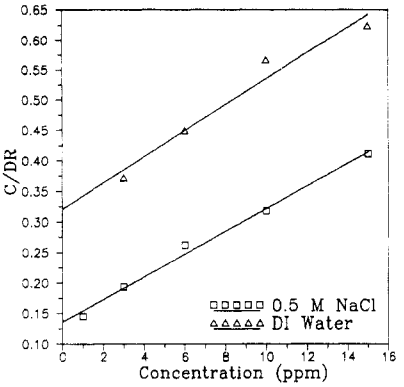

Figure 14. C/DR versus C for DAPS-40 in deionized water (Δ) and 0.5 M NaCl (□) at T_w = 1122 dyn/cm² in the rotating-disk rheometer.

In 0.5 M NaCl, DAPS-10 is found to be the most efficient drag reducer (Δ = 5.68). The ability of this copolymer to switch between intramer and intramolecular ionic associations may provide an efficient mechanism for turbulent energy dissipation. However, an increase in the AMP-DAPS content to 40 mol % (DAPS-40) reduces DRE, and the Δ value drops from 5.68 to 1.95. In this case and others with high comonomer content, the number of the more hydrated acrylamide repeating units is insufficient to yield adequate chain extension in turbulence.

ATABAM 2.5–2.5 (Δ = 1.96) is found to be the most efficient low charge density polyampholyte. The DRE for ATABAM 15–15 (Δ = 1.54) is not much lower than that for ATABAM 2.5–2.5 despite the higher charge density, indicating that the intramolecular ionic associations may not be as strong in the ATABAM terpolymers. The high charge density polyampholyte, ATAS-50, has the poorest DRE (Δ = 0.45) due to strong intramolecular ionic associations and poorer polymers–solvent interaction. The ATASAM terpolymers are only slightly better than ATAS-50, with Δ values of 0.84 and 0.82. The ATAS and the ATASAM polymers may be too tightly associated to open on colliding with a microvortex and are perhaps incapable of undergoing the mechanism proposed in Figure 1.

In deionized water or at low solvent ionic strength, DAPS-10 (Δ = 4.64) remains the most efficient drag reducer. All polyampholytes that have the SO_3^- anion (i.e., ATAS-50, the ATASAM terpolymers, and the DAPS copolymers) have lower Δ values in deionized water or at low solvent ionic strength relative to those in 0.5 M NaCl. However, the polyampholytes that have the CO_2^- anion (i.e., the ATABAM terpolymers) possess higher Δ values at low solvent ionic strength relative to those in 0.5 M NaCl (Table 4).

Little's Universal Relationship for Drag Reduction. Little's relationship provides another technique to compare the drag reduction characteristics of different polymers. From the plot of C/DR versus C (Figure 14) as represented in eq 1, the DR_{max} can be obtained from the reciprocal of the slope, and the intercept when multiplied by the DR_{max} yields the intrinsic concentration ([C]). Good drag reducers exhibit low values of intrinsic concentration. In this section, we have studied the effect of polyampholyte molecular structure and solvation on the intrinsic concentration.

DAPS-10 has the lowest intrinsic concentration of 1.8 ppm in 0.5 M NaCl and 2.7 ppm in deionized water (Table 5). The ATABAM terpolymers in any solvent and DAPS-40 in 0.5 M NaCl have intrinsic concentrations between 4.5 and 7.8 ppm. The ATASAM terpolymers and ATAS-50 show relatively higher intrinsic concentrations, indicating that they are poorer drag reducers.

Table 5. Intrinsic Concentration and DR_{max} As Obtained from Little's Universal Relationship for Drag Reduction

polymer/solvent	[C] (ppm)	DR_{max} (%)	$[C][\eta] \times 10^3$
PEO/DI water	6.2	42.3	7.56
PAM/DI water	4.1	60.1	9.14
ATAS-50/0.1 M NaCl	31.1	14.5	14.00
ATASAM 5-5/0.5 M NaCl	10.7	33.2	9.20
ATASAM 10-10/0.5 M NaCl	9.2	30.3	8.19
ATABAM 2.5-2.5/0.5 M NaCl	4.5	53.5	5.40
ATABAM 2.5-2.5/DI water	7.5	51.0	3.15
ATABAM 15-15/0.5 M NaCl	6.6	57.2	9.17
ATABAM 15-15/0.05 M NaCl	7.8	56.1	3.90
DAPS-10/0.5 M NaCl	1.8	47.6	2.07
DAPS-10/DI water	2.7	49.5	2.48
DAPS-40/0.5 M NaCl	7.4	54.0	5.92
DAPS-40/DI water	15.0	46.7	6.00

Table 6. $([C][\eta])^{-1}$ and Δ Values for Different Polymer/Solvent Systems

polymer/solvent	$([C][\eta])^{-1}$	Δ
PEO/DI water	132	1.00
PAM/DI water	109	1.37
ATAS-50/0.1 M NaCl	71	0.29
ATASAM 5-5/0.5 M NaCl	109	0.84
ATASAM 10-10/0.5 M NaCl	122	0.82
ATABAM 2.5-2.5/0.5 M NaCl	185	1.96
ATABAM 2.5-2.5/DI water	317	3.46
ATABAM 15-15/0.5 M NaCl	109	1.54
ATABAM 15-15/0.05 M NaCl	256	3.05
DAPS-10/0.5 M NaCl	483	5.68
DAPS-10/DI water	403	4.64
DAPS-40/0.5 M NaCl	169	1.95
DAPS-40/DI water	167	1.62

Polymer-solvent interaction also has a large effect on the intrinsic concentration. DAPS-40 (Table 5) has a [C] value of 7.4 ppm in 0.5 M NaCl, but in deionized water the [C] increases to 15.0 ppm. A more collapsed conformation leads to lower hydrodynamic volume as a result of intramolecular ionic associations which lessen the amount of water associated with the chain. Similarly, ATABAM 2.5-2.5 exhibits an increase in [C] from 4.5 to 7.5 ppm with decreasing solvent ionic strength.

Correlation between Little's Relationship and the Δ Parameter. Since the intrinsic concentration is very sensitive to the polymer molecular weight[11] as well as hydrodynamic volume (as discussed in this paper and refs 7 and 8), we have modified the intrinsic concentration by multiplying by the intrinsic viscosity, reasoning that $([C][\eta])^{-1}$ should scale with our Δ parameter. The $([C][\eta])^{-1}$ values for different polyampholytes in solvents of varying ionic strength are reported in Table 6 along with the Δ values. For the polyampholytes, plotting $([C][\eta])^{-1}$ versus Δ (Figure 15) yields a linear relationship with a correlation coefficient of 0.9865.

Correlation with Parameters from Existing Theories. Walsh's Parameter. Figure 16 is a plot of percent drag reduction as a function of $[\eta]^2CM$. From eq 3 the relationship between $[\eta]^2CM$ and the Walsh parameter, H, can be obtained. Although this relationship was developed for pipe flow, a Walsh-type parameter should also hold in rotating-disk geometry for conditions where τ_w is known.[2,3] In our experiments with polyampholytes, scatter of less than a decade is observed at the inflection point of the S-shaped curve from Figure 16. This scatter is likely due to the diverse structures of the polyampholytes and the resulting differential interaction with water. It is worth noting that the scatter in Figure 16 is not as pronounced as that seen with water-soluble polyelectrolytes reported earlier.[3]

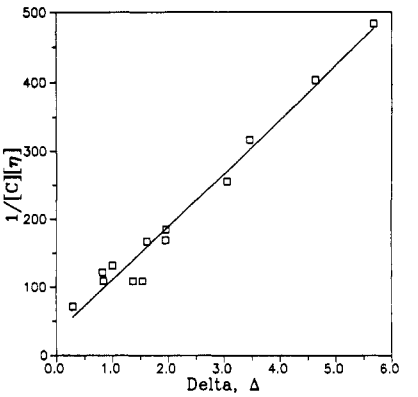

Figure 15. $1/[C][\eta]$ versus Δ to study the correlation between Little's intrinsic concentration and the Δ parameter.

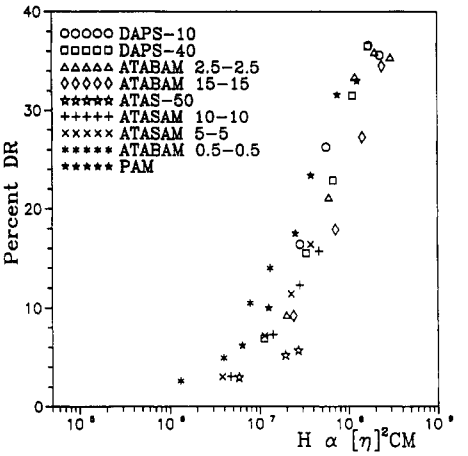

Figure 16. Percent DR versus $[\eta]^2CM$ for various polyamopholytes in 0.5 M NaCl at $T_w = 1122$ dyn/cm² in the rotating-disk rheometer.

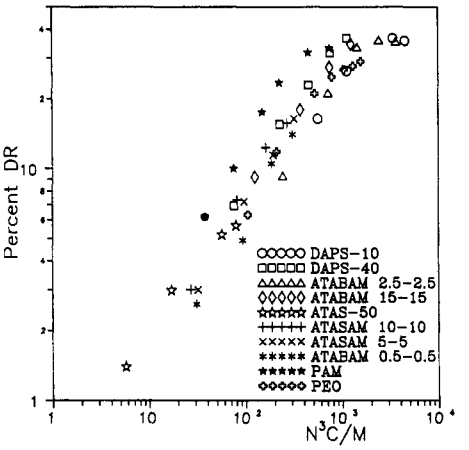

Figure 17. Percent DR versus N^3C/M for various polyampholytes in 0.5 M NaCl at $T_w = 1122$ dyn/cm² in the rotating-disk rheometer.

Ryskin's Parameter. Figure 17 illustrates the relationship between percent drag reduction in the rotating-disk geometry and N^3C/M for all polymers in 0.5 M NaCl. The experimentally known N^3C/M or N^2C/Ma (since $M = M_aN$) may be related to the parameter ζ_{turb} given in eq 4. Since the length of the repeating unit, a, is known, the ratio of the chain length to that of the fully extended chain, α, can be estimated as long as measurements are under the same flow conditions.

It should be mentioned that Ryskin developed his theoretical relationship for tube flow, so the α value experimentally determined in tube flow might be expected to differ from that determined in the rotational mode.

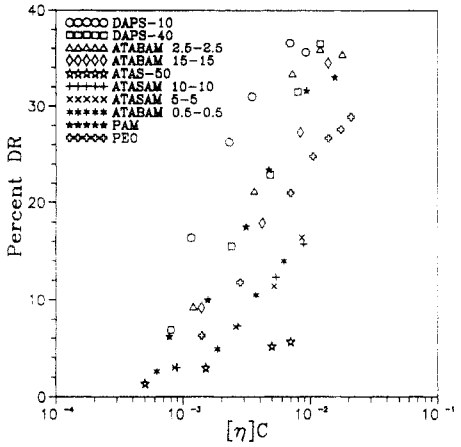

Figure 18. Percent DR versus $[\eta]C$ for different polyampholytes in 0.5 M NaCl at T_w = 1122 dyn/cm² in the rotating-disk rheometer.

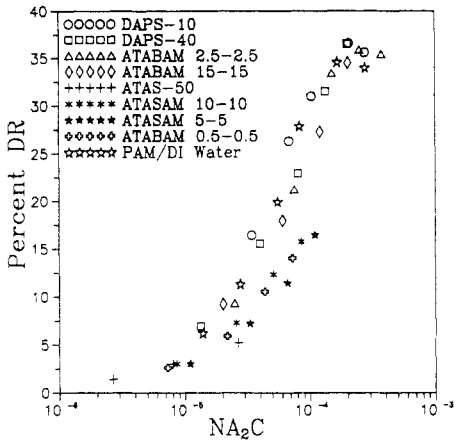

Figure 19. Percent DR versus NA_2C for various polyampholytes in 0.5 M NaCl at T_w = 1122 dyn/cm² in the rotating-disk rheometer.

However, the reasonably small degree of scatter in the rotational data reported here indicates a nearly constant value of α for these similar polymer structures. We have pointed out previously large changes in α for polymers with widely differing structures and degrees of hydration but constancy in α with similar polymer microstructure.[2-4] Since α is important in relating N^3C/M to ζ_{turb} in a given flow geometry, solvent associated with the coil (and changes thereof) and longer range interactions during extension merit further consideration. In a "yo-yo" model of the type proposed by Ryskin such interactions might be partially accounted for by adjusting the bond length or by using appropriate persistence length elements for the contributing segments.

Comparisons of Drag Reduction as a Function of Volume Fraction. Figure 18 is a plot of % DR versus hydrodynamic volume fraction ($[\eta]C$) for the polyampholytes in 0.5 M NaCl. The differences in polymer structure lead to a substantial scatter on this plot. Many researchers have previously reported that all polymers at the same volume fraction yield the same value of drag reduction. However, it is likely that the drag reduction performance also depends on the efficiency with which a polymer coil can interact with the microdisturbances in turbulent flow. Therefore, one has to resort to volume fraction normalization for a more accurate picture of relative drag reduction efficiency.

Empirical Relationship Based on Solvation Parameters. A good correlation was reported in previous publications[7,8] between percent drag reduction and NA_2C (N = degree of polymerization, A_2 = second virial coefficient from light scattering experiments, and C = polymer concentration). Such a correlation might be expected due to the inclusion of three important molecular parameters: N, the polymer length; A_2, a measure of polymer–solvent interaction; and C, the concentration of polymer molecules. As before, a satisfactory correlation between % DR and NA_2C was obtained (Figure 19). It should be noted that only the polyampholytes with poor drag reduction efficiencies ($\Delta < 1$) deviate from the main curve. This empirical relationship also highlights the important role played by solvent (as reflected by A_2 values) in drag reduction.

Conclusions

The drag reduction behavior of several well-characterized, water-soluble polyampholytes has been studied. Three classes of polyampholytes have been examined: high and low charge density polyampholytes and betaine copolymers with sulfonate moieties. A dependence of drag reduction effectiveness on copolymer structure, composition, and solvation has been observed. All polyampholytes exhibited higher intrinsic viscosity and % DR with increasing solvent ionic strength. The betaine copolymers have the best drag reduction properties and the high charge density polyampholyte the poorest. The low charge density polyampholytes exhibit intermediate drag reduction effectiveness. The acrylamide copolymers are more resistant to shear degradation than PEO. Experimental drag reduction data for all copolymers can be empirically related to fundamental hydrodynamic parameters utilizing Δ, $1/[\eta][C]$, or NA_2C. Absolute drag reduction observations combined with such empirical relationships of drag reduction efficiency give the synthetic chemist important clues to tailoring optimal systems. The agreement between predictive theoretical models and experimentally derived empirical relationships is still lacking. However, new models incorporating the role of changes in solvation and polymer conformation in turbulent flow may allow better agreement of experiment with theory.

Acknowledgment. Financial support from the U.S. Department of Energy, the Office of Naval Research, and the Defense Advanced Research Projects Agency is gratefully acknowledged.

References and Notes

(1) Toms, B. A. *Proc. Int. Cong. Rheol.* **1949**, *2*, 135.
(2) Morgan, S. E. Ph.D. Dissertation, The University of Southern Mississippi, Hattiesburg, MS, 1988.
(3) McCormick, C. L.; Hester, R. D.; Morgan, S. E.; Safieddine, A. M. *Macromolecules* **1990**, *23*, 2124.
(4) McCormick, C. L.; Hester, R. D.; Morgan, S. E.; Safieddine, A. M. *Macromolecules* **1990**, *23*, 2132.
(5) Mumick, P. S.; Morgan, S. E.; McCormick, C. L. *Polym. Prepr. (Am. Chem. Soc., Div. Polym. Chem.)* **1989**, *30* (2), 256.
(6) Mumick, P. S.; Welch, P. M.; Hester, R. D.; McCormick, C. L. *Polym. Prepr. (Am. Chem. Soc., Div. Polym. Chem.)* **1992**, *33* (2), 337.
(7) Mumick, P. S. Ph.D. Dissertation, The University of Southern Mississippi, Hattiesburg, MS, 1993.
(8) Mumick, P. S.; Hester, R. D.; McCormick, C. L. Water-Soluble Copolymers. 55. *N*-Isopropylacrylamide-*co*-Acrylamide Copolymers in Drag Reduction: Effect of Molecular Structure, Hydration, and Flow Geometry on Drag Reduction Performance, submitted for publication.
(9) Virk, P. S.; Merrill, E. W.; Mickley, H. S.; Smith, K. A.; Mollo-Christensen, E. L. *J. Fluid Mech.* **1967**, *30* (2), 305.
(10) Little, R. C. *J. Colloid Interface Sci.* **1971**, *37* (4), 811.
(11) Ting, R. Y.; Little, R. C. *J. Appl. Polym. Sci.* **1973**, *17*, 3345.

(12) Walsh, M. Ph.D. Thesis, California Institute of Technology, 1967.
(13) Lumley, J. L. *J. Polym. Sci., Macromol. Rev.* **1973**, *7*, 263.
(14) Ryskin, G. *J. Fluid Mech.* **1987**, *178*, 423.
(15) Ryskin, G. *Phys. Rev. Lett.* **1987**, *59* (18), 2059.
(16) Virk, P. S. *AIChE J.* **1975**, *21* (4), 625.
(17) Morgan, S. E.; McCormick, C. L. *Prog. Polym. Sci.* **1990**, *15*, 507.
(18) Salazar, L. C. Ph.D. Dissertation, The University of Southern Mississippi, Hattiesburg, MS, 1991.
(19) McCormick, C. L.; Salazar, L. C. *Macromolecules* **1992**, *25*, 1896.
(20) McCormick, C. L.; Salazar, L. C. *Polymer* **1992**, *33*, 4384.
(21) McCormick, C. L.; Salazar, L. C. *J. Appl. Polym. Sci.* **1993**, *48*, 1115.
(22) McCormick, C. L.; Salazar, L. C. *Polymer* **1992**, *33*, 4617.
(23) Dickerson, J. P. Ph.D. Dissertation, The University of Southern Mississippi, Hattiesburg, MS, 1993.
(24) Isaacs, N. S. In *Physical Organic Chemistry*; John Wiley & Sons: New York, 1987; p 239.
(25) Pearson, R. G. *J. Am. Chem. Soc.* **1963**, *85*, 3533.